

RESEARCH ARTICLE

Fractal-structured multifocal intraocular lens

Laura Remón¹, Salvador García-Delpech², Patricia Udaondo², Vicente Ferrando^{3,4}, Juan A. Monsoriu³, Walter D. Furlan^{4*}

1 Departamento de Física Aplicada, Universidad de Zaragoza, Zaragoza, Spain, **2** Ophthalmology Department, Hospital Universitario La Fe, Valencia, Spain, **3** Centro de Tecnologías Físicas, Universitat Politècnica de València, Valencia, Spain, **4** Departamento de Óptica y Optometría y Ciencias de la Visión, Universitat de València, Burjassot, Spain

* walter.furlan@uv.es



Abstract

In this work, we present a new concept of IOL design inspired by the demonstrated properties of reduced chromatic aberration and extended depth of focus of Fractal zone plates. A detailed description of a proof of concept IOL is provided. The result was numerically characterized, and fabricated by lathe turning. The prototype was tested in vitro using dedicated optical system and software. The theoretical Point Spread Function along the optical axis, computed for several wavelengths, showed that for each wavelength, the IOL produces two main foci surrounded by numerous secondary foci that partially overlap each other for different wavelengths. The result is that both, the near focus and the far focus, have an extended depth of focus under polychromatic illumination. This theoretical prediction was confirmed experimentally by means of the Through-Focus Modulation Transfer Function, measured for different wavelengths.

OPEN ACCESS

Citation: Remón L, García-Delpech S, Udaondo P, Ferrando V, Monsoriu JA, Furlan WD (2018) Fractal-structured multifocal intraocular lens. PLoS ONE 13(7): e0200197. <https://doi.org/10.1371/journal.pone.0200197>

Editor: José M. González-Méijome, Universidade do Minho, PORTUGAL

Received: October 4, 2017

Accepted: June 21, 2018

Published: July 9, 2018

Copyright: © 2018 Remón et al. This is an open access article distributed under the terms of the [Creative Commons Attribution License](https://creativecommons.org/licenses/by/4.0/), which permits unrestricted use, distribution, and reproduction in any medium, provided the original author and source are credited.

Data Availability Statement: All relevant data are within the paper and its Supporting Information files.

Funding: This study was supported by Ministerio de Economía y Competitividad www.mineco.gob.es/ FEDER (Grant DPI2015-71256-R) and by Generalitat Valenciana www.ceice.gva.es/web/ciencia (Grant PROMETE0II-2014-072), Spain.

Competing interests: LR, WDF and JAM co-inventors of a patent application related to this study, Multifocal ophthalmic lens and method for obtaining the same. ES Patent 2011/070559; PCT/

Introduction

With millions of procedures carried out each year, cataract surgery is one of the most common operations nowadays, with an increasing rate of growth worldwide. Cataracts frequently start to develop in people as they get older, producing a loss of vision that can only be corrected by surgery. In cataract surgery, the crystalline lens that has become cloudy, is removed and replaced with an intraocular lens (IOL). Many of the IOLs that are currently in the market are bifocals designed to provide good distance and near vision. Depending on the lens design, several addition powers, distribution of energy between the foci, and depth of focus are available with different models [1]. However, the main shortcoming of current bifocals is their low performance at intermediate distances [2,3]. Therefore, due to the patient's demand, nowadays there is a trend to design new IOLs that provide also good intermediate vision, which is important for performing several daily tasks (such as, viewing the dashboard in a car, cooking, using computers and smartphones, etc). This tendency was initiated a few years ago with the introduction of the low-addition bifocal IOLs [3,4], intended to match the lens addition with the patient's intermediate focus. Diffractive trifocal IOLs were introduced later with the aim to offer simultaneously two different additions, one (+3.50D), for near vision and the other (+1.75D) for intermediate vision [5].

ES2014/000094, WO Patent 2012/028755 A1. Inventors: Walter Daniel Furlan, Pedro ANDRÉS, Amparo PONS, Genaro Saavedra, Juan Antonio MONSORIU, Fernando GIMÉNEZ, Laura REMÓN, Arnau CATALAYUD, Manuel RODRÍGUEZ, Juan Luis Rojas, Eva Larra, Pedro José Salazar. Original Assignee: Universitat De València, Universitat Politècnica De València, Aji Ophthalmic, SA. Priority date: 2013-06-10. There are no further patents, products in development or marketed products to declare. This does not alter our adherence to all the PLOS ONE policies on sharing data and materials, as detailed online in the guide for authors.

Following the above mentioned trend, more recently both, refractive, and diffractive, extended depth of focus (EDOF) designs have been developed with the intention to provide a “continuous” range of vision, from far to intermediate-near vision. In the first group, the refractive zones in the lens, having different powers, can be either: rotationally symmetric in different annuli, like the M-flex multifocal IOL (Rayner, Hove, United Kingdom), or angularly segmented, like the Lentis M-Plus (Oculentis GmbH, Berlin, Germany), and the SBL-3 IOL (Lenstec, St. Petersburg, USA). In the second group, two new diffractive multifocal IOLs were designed; the Mini WELL Ready (SIFI MedTech, Catania, Italy) and the TECNIS Symphony ZXR00 (Abbott Laboratories, Illinois, USA). These last two models are based on different optical principles. The Mini WELL Ready presents different amounts of spherical aberration in two concentric zones in the central part of the lens [6]. The TECNIS Symphony ZXR00 is based on the combined correction of the spherical and longitudinal chromatic aberrations of the eye [7]. In truth, as recently reported by Millán and Vega [8], the in vitro EDOF performance of this IOL is highly wavelength-dependent. On the other hand, a previous study [9] showed that, even for monochromatic light (545 nm), the EDOF of both diffractive designs is also pupil-dependent.

In this work we present a conceptually new multifocal IOL design intended to provide good vision at multiple distances. A proof of concept of a multifocal IOL was constructed following a hybrid diffractive-refractive design [10] that provides EDOF and low chromatic aberration simultaneously. These properties are inherited from Fractal zone plates (FZPs) and devil's lenses [11–15] which are diffractive lenses that have multiple foci with unique self-replicating fractal structure around a main focus. Under white light illumination, different wavelengths come to focus at different distances, but with certain degree of overlapping that results in an EDOF with reduced chromatic aberration. The fractal design can also be used to modify both the number and the relative intensities of the foci. FZPs have been successfully employed in several areas, ranging from spectral-domain optical coherence tomography [16] to terahertz technology [17]. Here we expand the range of applications of fractal lenses by presenting a novel design of multifocal IOL developed using the fractal triadic Cantor set. This set is used to modify the pure spherical profile of a monofocal IOL so that the resulting refractive-diffractive hybrid design has two main powers, intended for distance and near vision, with EDOF for intermediate vision. Thus, we called it: Fractal Intraocular Lens (FIOL). The FIOL proof of concept was numerically evaluated, and tested in vitro on an optical bench.

Intraocular lens design and construction

FZPs are characterized by the distribution of the annular diffractive zones they have, which, in spite of being periodic along the square root of the radial coordinate, like a Fresnel zone plate is, it follows the sequence of a given fractal Cantor set. In previous works we have demonstrated that FZPs can be constructed following any class of Cantor Functions, including polyadic Cantor sets [18] and functions with variable lacunarity [19]. As a proof of concept, our first FIOL design is based on the simplest Cantor set shown in Fig 1a, which is called triadic Cantor set. The first step in the construction procedure of this set, consists in defining a straight-line segment of unit length, called *initiator* (stage $S = 0$). Next, at stage $S = 1$, the *generator* of the set is created by dividing the segment into 3 equal sub segments of length $x = 1/3$ and removing the central one. This procedure is repeated for the subsequent stages, $S = 2, 3, \dots$, on each sub segment. Then, a change of variables $r = b\sqrt{x}$ is performed to define the extension of the concentric zones in the FIOL, up to a given lens radius b (see Fig 1b). In this way, our design alternates annular zones that follows a fractal distribution along the square of the radial coordinate. Note that the total number of sub-segments in each stage of the Cantor set is $N = 3^S$; and that

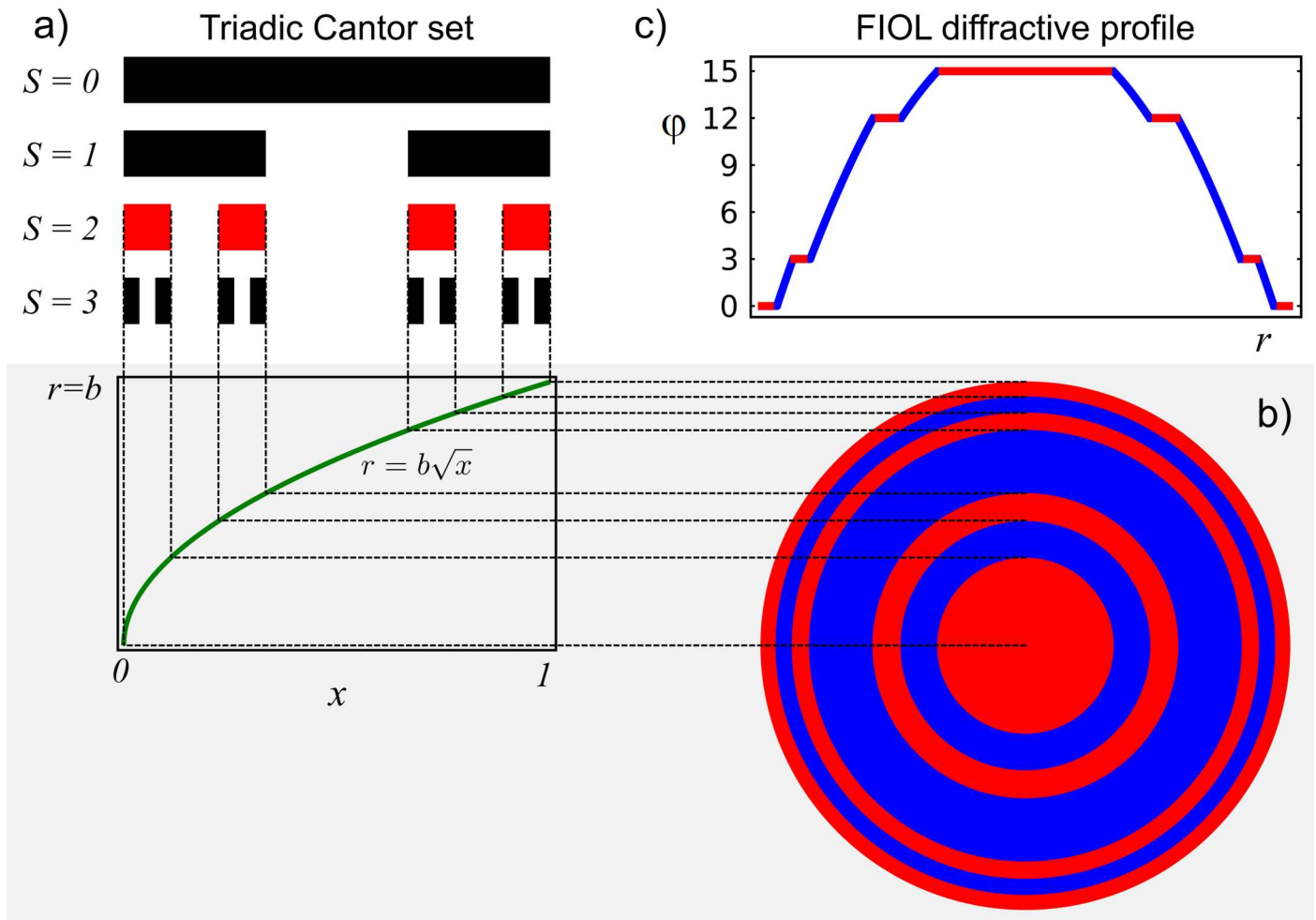


Fig 1. FIOLE design. a) Top left: Triadic Cantor set developed up to three steps, $S = 3$; b) FIOLE fractal zones distribution for $S = 2$, obtained through the coordinate transformation $r = b\sqrt{x}$ c) FIOLE diffractive profile obtained with $K = 3$ (see the main text for details).

<https://doi.org/10.1371/journal.pone.0200197.g001>

each one of them, with an extension $x = 1/3^S$, has a corresponding Fresnel zone in the FIOLE fractal zone distribution. The next step in the FIOLE design process is to define the phase profile of these zones in such a way that the first diffraction order of this structure will produce the near FIOLE power. One solution is to employ a conventional kinoform profile in which the facets of the lens produce a 2π phase shift for the design wavelength λ . These lenses, known as devil's lenses, have a focal distance that depends on the number of the above mentioned Fresnel zones, through the S parameter as $f = b^2/2 \lambda_0 3^S$ [12]. In this way, the FIOLE addition (Ad), i.e.; the difference between the near and far powers results:

$$Ad = \frac{2 \lambda_0 3^S}{b^2} \tag{1}$$

However, for our purposes is convenient to introduce one more degree of freedom in the FIOLE design, to cover a wide range of Ad s with the same fractal structure. By using the concept of harmonic diffractive lens [20], this is possible if the phase difference introduced in each

Fresnel zone is $\varphi = 2\pi K$, being K a positive integer number. Additionally, to facilitate the lens construction, the above mentioned phase differences can be “staked” sequentially from the periphery to the center avoiding a saw tooth (kinoform) profile. In this way, in each Fresnel zone, the increment of height corresponding to the desired Ad is $\Delta h = K \lambda_0 / (n - n')$, where n and n' are the refractive index of the lens material and the surrounding FIOI media (aqueous humor) respectively. Therefore, the FIOI Ad can be expressed alternatively as:

$$Ad = \frac{2 \cdot 3^S \Delta h (n - n')}{b^2} \tag{2}$$

As reported in Ref [20], lenses constructed in this way have hybrid properties of both refractive and diffractive lenses.

Returning to Fig 1, if we choose $S = 2$ in the Fractal structure, and considering a “center far” FIOI design, the Ad phase profile is incremented in the “blue” rings in Fig 1b). For $K = 3$ the final result is shown in Fig 1c).

A FIOI prototype was designed to be constructed in Polymethyl methacrylate (PMMA) (refractive index $n = 1.493$ at the design wavelength $\lambda_0 = 555 \times 10^{-9} \text{m}$); with dioptric power 19.5 D. The radii of curvature for the front and back surfaces were $12.42 \times 10^{-3} \text{m}$, and $22.89 \times 10^{-3} \text{m}$ respectively. The proof of concept FIOI was conceived with the fractal profile in the anterior surface of the lens providing an $Ad = +3.5 \text{D}$. This value was obtained with: $S = 2$, $K = 3$, and $b = 2.92 \times 10^{-3} \text{m}$ using Eq (1). See Fig 2a.

The multifocal FIOI was manufactured by a lathe-milling process (Optoform40, Sterling Ultra Precision, Largo FL, USA), similar to that for standard monofocal IOLs, but without the polishing step. Differences between the theoretical design and the constructed FIOI profiles were lower than 0.1 mm as measured with an optical non-contact profilometer (PLμ 2300, SENSOFAR, Terrassa, Spain). An interferometric image (PMTF, Lambda-X, Nivelles, Belgium) of the manufactured FIOI is shown in Fig 2b). The haptic for the prototype was chosen as shown in the figure, simply to facilitate the lens handling during its assessment (the design of the lens haptic has no influence on its optical properties and it was beyond the scope of this work).

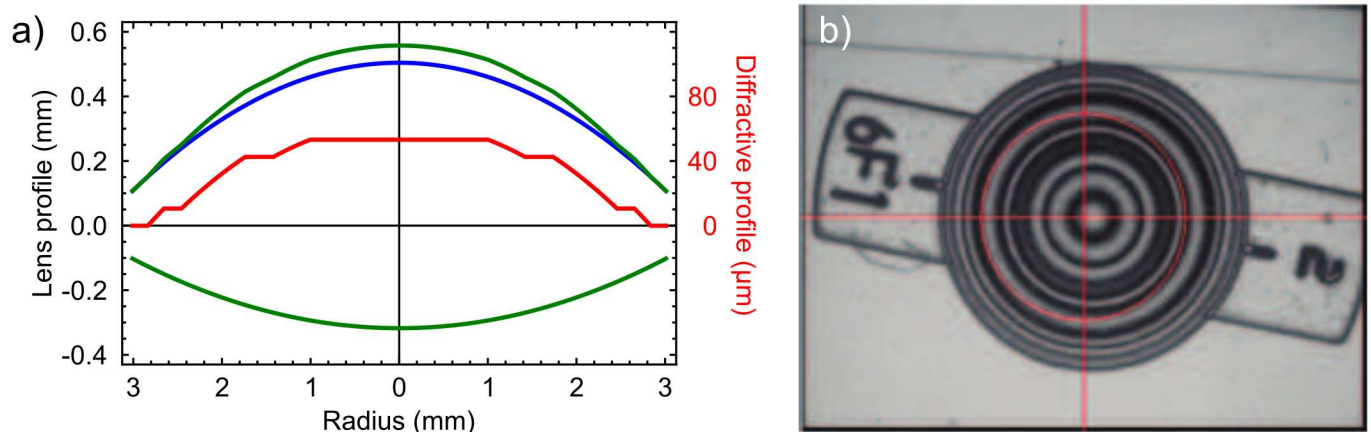


Fig 2. FIOI proof of concept. a) Theoretical profiles of the anterior and posterior FIOI surfaces (green line). The red line is the diffractive profile of the FIOI, designed with $S = 2$ and $K = 3$ (magnified X5 in the vertical direction in order to show the relative heights of the diffractive steps); this profile was superimposed to a pure spherical profile of a monofocal IOL radius $r = 12.42 \text{mm}$ (blue line). b) Interferometric image of the constructed lens.

<https://doi.org/10.1371/journal.pone.0200197.g002>

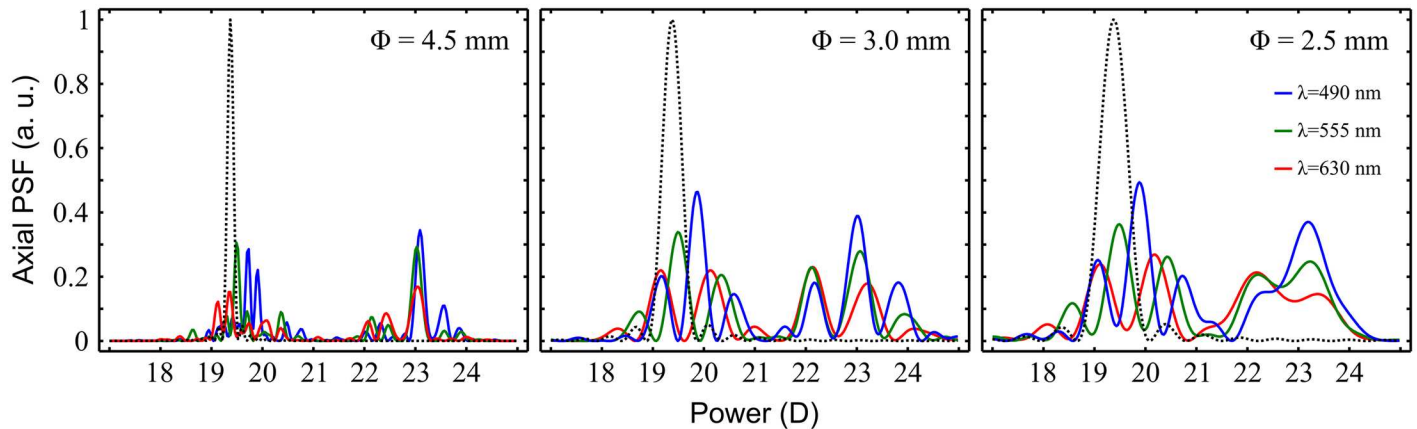


Fig 3. Theoretical axial PSFs provided by a FIOIOL. Results for a lens with distance power 19.5 D ($A_d = +3.5D$) with different pupil diameters (Φ) and three wavelengths: $\lambda = 490$ nm (blue line); $\lambda = 555$ nm (green line), and $\lambda = 630$ nm (red line). In each plot, the dotted lines are the PSFs ($\lambda = 555$ nm) of a monofocal 19.5 D IOL.

<https://doi.org/10.1371/journal.pone.0200197.g003>

Numerical validation of the FIOIOL design

For the theoretical characterization of the lens, wavefront propagation and Fourier analysis were performed numerically using Fresnel diffraction theory. In the simulations, it is assumed that the lens is immersed in aqueous humor (refractive index: $n' = 1.336$). To assess its focusing properties, the Point Spread Function (PSF) provided by the FIOIOL, was computed at different axial positions for different pupil diameters and wavelengths.

The numerical axial PSFs provided by the designed FIOIOL for different wavelengths (λ) and three different pupil diameters (Φ) are shown in Fig 3 in comparison with the irradiances of a monofocal IOL with the same dioptric power 19.5 D and the same shape factor. As can be seen, for each wavelength the FIOIOL produces two main foci surrounded by numerous secondary foci that partially overlap each other for different wavelengths. The result is that both, the near and far foci, have an EDOF under polychromatic illumination.

Additionally, another objective metric, highly correlated with the visual acuity: the theoretical visual Strehl ratio computed in frequency domain (MTF method) [21], or simply: the Visual MTF (VMTF), was computed for the two main foci (far and near), with different pupil sizes (see Fig 4). As can be seen, despite of being pupil-dependent, the FIOIOL enhanced the far vision, especially with small pupil sizes.

Experimental results

The optical performance of the FIOIOL was experimentally tested in vitro with a custom made image forming system that allows the measurement of the polychromatic TF-MTF. A schematic illustration of the experimental system is shown in Fig 5. This setup is similar to one presented previously [22] containing an ISO eye model [23], except for the artificial cornea which has been removed to obtain a better through the focus resolution. The illumination system consists of a white LED (Luxeon™, V Portable, Alberta, Canada). A band-pass filter was placed behind it to assess the FIOIOL performance with different wavelengths. The beam was collimated by the lens L1 (focal length: 50 mm). The test object, a grating target of frequency $\nu = 5$ lp mm⁻¹, was mounted on a stepping motorized translation stage (travel range 300 mm, accuracy: ± 5 μ m). The Badal lens L2 was an achromatic lens of focal length: 160 mm. The FIOIOL prototype was placed in different holders with different pupil sizes and immersed in a wet cell with saline solution. An 8-bit CMOS camera (EO-5012C; Edmund Optics, Illinois, USA);

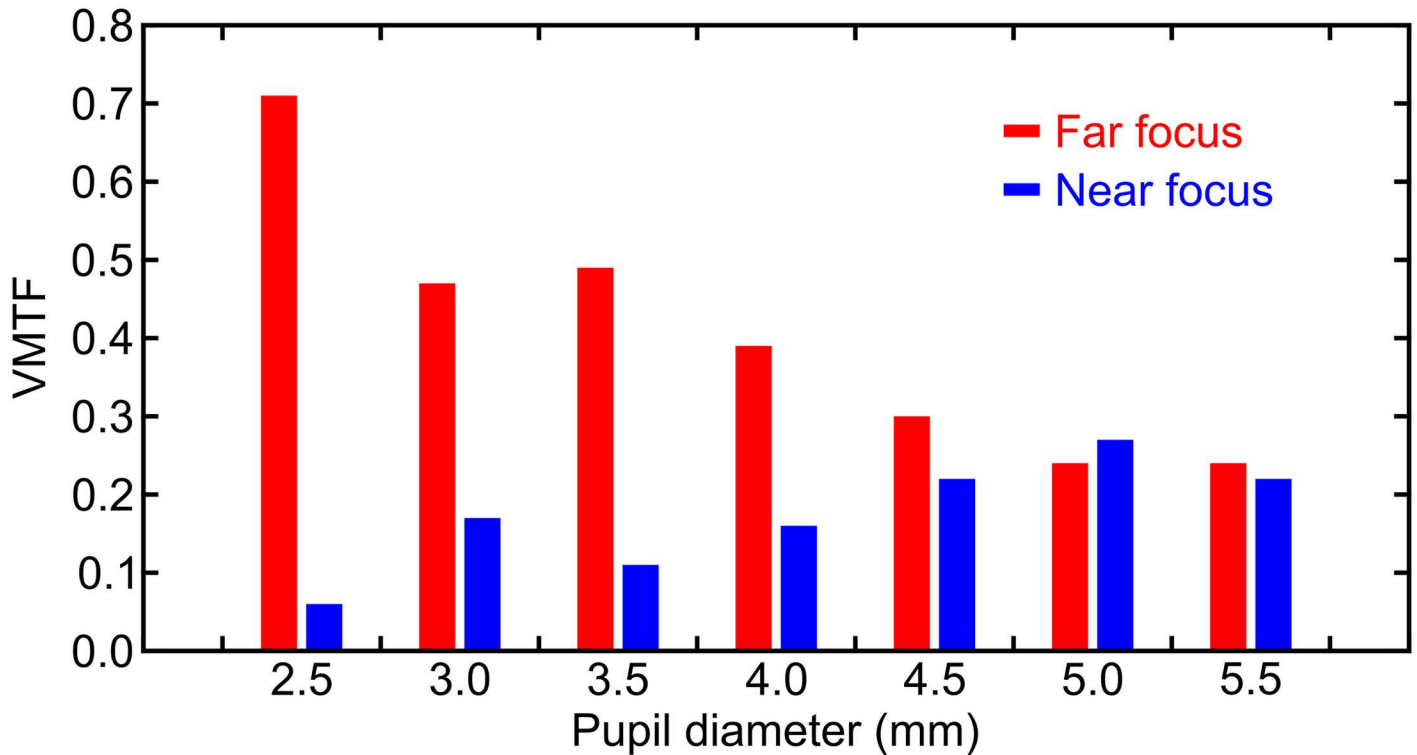


Fig 4. Theoretical visual MTF for the different pupil sizes. These results were computed from the Fourier transform of the monochromatic PSF (the MTF) for the design wavelength $\lambda_0 = 555$ nm, weighted by the neural contrast sensitivity function [21].

<https://doi.org/10.1371/journal.pone.0200197.g004>

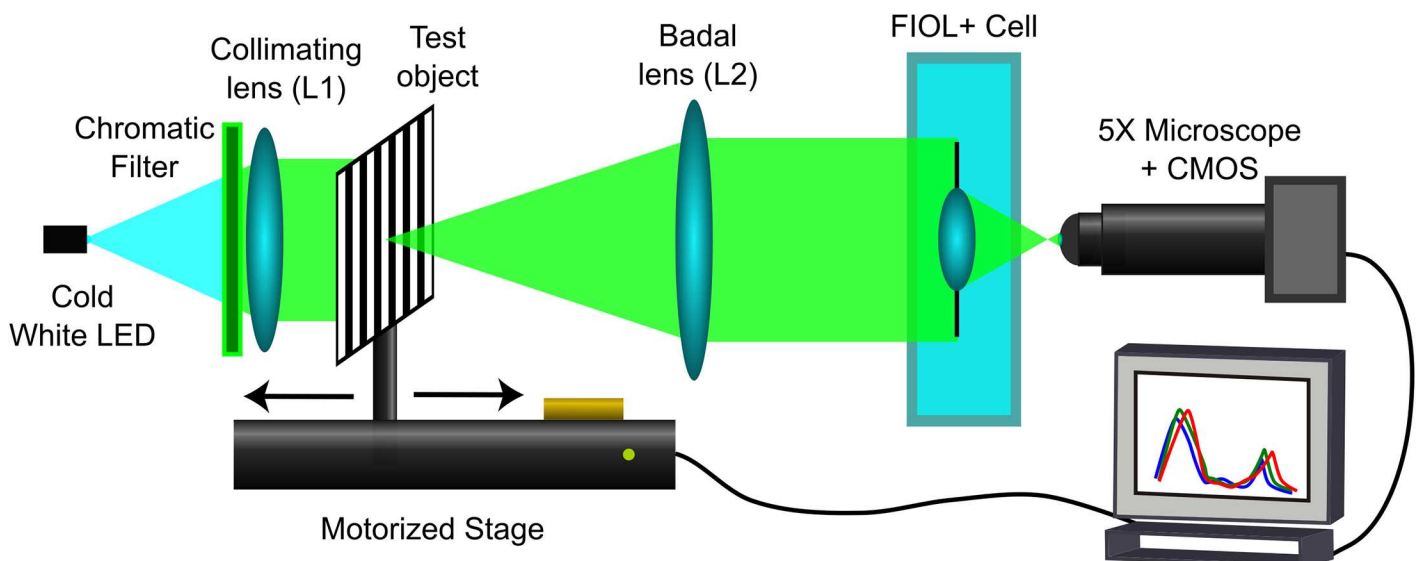


Fig 5. Optical bench for in-vitro testing. The object test was mounted on a linear translation stage. As the FIO+ to be tested was placed at the image focal plane of L2 we called it: Badal lens. This configuration guaranteed that the angle subtended by the test object, and consequently the spatial frequency assessed in the TF-MTF, was constant for all vergences and equal to 14 cpd. The retinal image was recorded with an X5 microscope and a CMOS camera.

<https://doi.org/10.1371/journal.pone.0200197.g005>

attached to an X5 microscope (focused on the far focal plane of the FIOI) was used to capture the image of object for different vergences. The spatial frequency of the grating corresponds to an object of size 20/40 (0.3 logMAR) in a visual acuity (VA) chart, and is constant at all object vergences.

The object plane was displaced along the optical axis to generate vergences, ranging from -1D to +6D in steps of 0.04D. Vergences were measured from the object focal plane of L2, being positive for displacements towards L2, and negative for displacements in the opposite direction. For each position of the object, the retinal image was stored and analyzed in a totally automatic procedure. The movements of the translation stage and the processing of the retinal images were controlled by custom software programmed in LabView. The MTF for each object vergence was obtained from the calculation of the loss of contrast of the image of the test object. A detailed description of the setup performance can be found elsewhere [22].

Fig 6 shows the experimental TF-MTF, measured for an aperture of 4.5 mm and three different wavelengths: 490 nm, 560 nm, and 630 nm.

As predicted by the theoretical axial PSF (Fig 3) the TF-MTF curve presents several peaks for the different wavelengths distributed along the whole range of vision. Finally, for evaluating the polychromatic imaging in the eye, these monochromatic (RGB) MTFs were combined numerically, weighted by the spectral sensitivity function of the human eye under daylight conditions $V(\lambda)$ [24], the spectral content of the illumination source, and the FIOI material transmission. The result, represented by the black line represents in Fig 6., is a compound focal volume with EDOF.

Discussion and conclusions

In the present study, a new hybrid diffractive/refractive multifocal IOL was presented and evaluated in-vitro. The theoretical design of this lens is based on a general method [10] that includes diffractive profiles having different aperiodic distributions of annular zones. Here, a proof of concept was developed using the triadic Cantor set fractal distribution. In our design, we have found that the Cantor function with $S = 2$ and with $K = 3$, provides the simplest multifocal structure for a FIOI, in which the refractive and diffractive properties of the lens are optimized. In fact, as shown in Ref. [11], as S becomes larger in a FZP, an increasing number of subsidiary (diffractive) foci are generated, which means that, in designs with $S = 3$, the diffractive effects would become more predominant over the refractive ones, which would result in a loss of light efficiency compared to designs with $S = 2$.

The proposed lens (FIOI) is a center-distance EDOF design that provides a clear dominance of the far focus with different pupil sizes. In fact, the theoretical results presented in Fig 4, show that despite of some degree of pupil-dependence, the highest value of MTF was achieved for the far focus for almost all considered pupil diameters. Opposite results, i.e.; lenses with a clear dominance of the near focus, were obtained in a preliminary study [25] (in Spanish). In that work we investigated the performance of a design in which the zones were interchanged with respect to those shown in Fig 1.

The polychromatic behavior of the lens was assessed both theoretically, and experimentally in a dedicated optical setup. We have shown that, thanks to its hybrid nature, the FIOI has two principal foci, intended to provide far and near vision, and a series of secondary foci around them, that give an EDOF to each main focus, improving intermediate vision. Moreover, thanks to these secondary foci, the FIOI has a reduced chromatic aberration because under polychromatic illumination there is a partial overlapping between them for the different wavelengths (see Fig 3). In the analysis of the experimental results reported in Fig 6. It should be taken into account that both, the cutoff frequency, and the values of the MTF obtained in

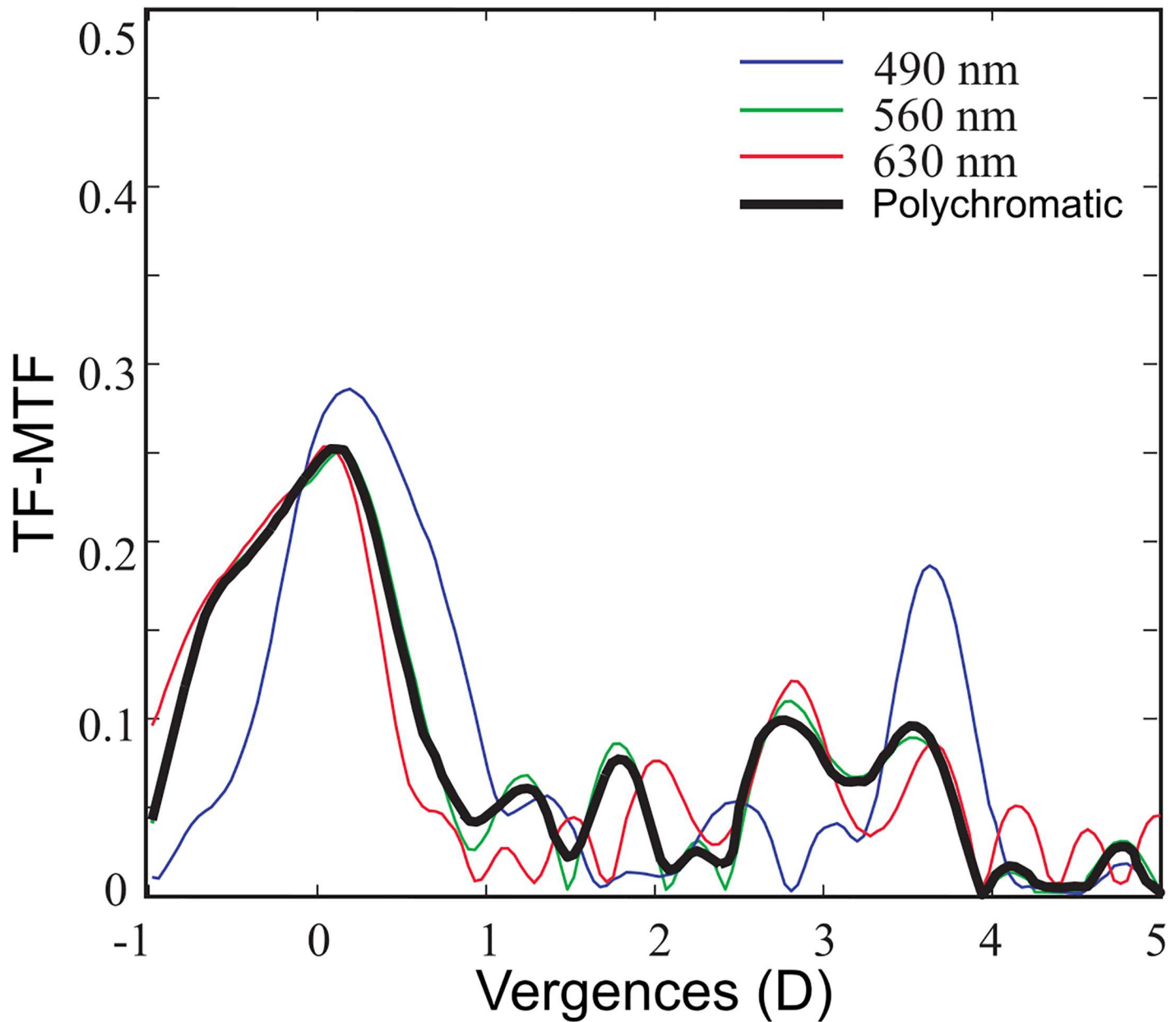


Fig 6. Experimental TF-MTF. FIOI's TF-MTF for 14 cpd obtained in the optical bench (Fig 6) with 4.5 mm pupil for different wavelengths. Zero defocus corresponds to far vision.

<https://doi.org/10.1371/journal.pone.0200197.g006>

the test bench for the FIOI without cornea are lower than the cutoff frequency provided by an artificial eye with the cornea lens and the FIOI [25]. Furthermore, because of the hybrid nature of the far and near foci, and based on the results recently reported by Nakajima et al. [26] for monofocal refractive IOLs, it can be expected that the visual performance of eyes implanted with FIOIs will be similar to that of phakic eyes when some extent of higher-order aberration exists. At this point, it is important to note that this behavior is different from other diffractive multifocal IOLs, which have elevated levels of chromatic aberration of opposite sign [8, 27].

We want to emphasize that the design parameters of the FIOI allow customization. In fact, a FIOI can be designed to match the patient's *Ad*, and visual needs; for instance: ratio between

the near and far intensities can be modified by the lacunarity in the Cantor set (see Fig. 3 Ref. [19]). This parameter also allows controlling the number of foci of the FIOL. Therefore, the flexibility in the FIOL design can be considered an advantage over other multifocal IOL models. Moreover, other fractal profiles can be used to address other particular needs.

Some limitations of this study will be addressed in the future. Further studies should involve other in vitro optical quality measurements of the FIOL, such as: the use of other (foldable) materials for the lens construction, and the effect on the merit functions (PSF, MTF, and TF-MTF) of the FIOL decentration and tilt [28]. Moreover, improvements in the reported results could be expected with different aspheric designs on the base lens intended to the correction of spherical aberration [29]. Finally, a clinical evaluation of patients who have had implantation of the FIOL is required to determine the visual impact of our design on the patient's quality of vision, particularly, to assess how the multifocal action of the lens affects the contrast sensitivity at several distances.

Supporting information

S1 Dataset. Axial PSFs data, computed at 0.03D intervals as represented in Fig 3.
(XLSX)

Acknowledgments

The authors are very grateful to AJL Ophthalmic S.A. (Spain) for manufacturing the FIOLs prototypes and to Laurent Malfaire (Lambda X, Belgium) for supplying the image shown in Fig 2a).

Author Contributions

Conceptualization: Juan A. Monsoriu, Walter D. Furlan.

Data curation: Laura Remón.

Formal analysis: Laura Remón, Vicente Ferrando, Juan A. Monsoriu, Walter D. Furlan.

Investigation: Laura Remón, Salvador García-Delpech, Patricia Udaondo, Juan A. Monsoriu, Walter D. Furlan.

Methodology: Patricia Udaondo, Walter D. Furlan.

Software: Vicente Ferrando.

Supervision: Salvador García-Delpech, Juan A. Monsoriu.

Writing – original draft: Walter D. Furlan.

References

1. Charman WN. Developments in the correction of presbyopia II: surgical approaches *Ophthalmic Physiol Opt.* 2014; 34: 397–426. <https://doi.org/10.1111/opo.12129> PMID: 24716827
2. Petermeier K, Messias A, Gekeler F, Szurman P. Effect of +3.00 diopter and +4.00 diopter additions in multifocal intraocular lenses on defocus profiles, patient satisfaction, and contrast sensitivity. *J Cataract Refract Surg.* 2011; 37: 720–726. <https://doi.org/10.1016/j.jcrs.2010.11.027> PMID: 21420598
3. Pepose JS, Wang D, Altmann GE. Comparison of through-focus image sharpness across five presbyopia-correcting intraocular lenses. *Am J Ophthalmol.* 2012; 154: 20–28. <https://doi.org/10.1016/j.ajo.2012.01.013> PMID: 22464368
4. Hayashi K, Manabe SI, Hayashi H. Visual acuity from far to near and contrast sensitivity in eyes with a diffractive multifocal intraocular lens with a low addition power. *J Cataract Refract Surg.* 2009; 35: 2070–2076. <https://doi.org/10.1016/j.jcrs.2009.07.010> PMID: 19969210

5. Gatinel D, Pagnouille C, Houbrechts Y, Gobin L. Design and qualification of a diffractive trifocal optical profile for intraocular lenses. *J Cataract Refract Surg*. 2011; 37: 2060–2067. <https://doi.org/10.1016/j.jcrs.2011.05.047> PMID: 22018368
6. Bellucci R, Curatolo M, A New Extended Depth of Focus Intraocular Lens Based on Spherical Aberration. *J Refract Surg*. 2017; 33: 389–394. <https://doi.org/10.3928/1081597X-20170329-01> PMID: 28586499
7. Artal P, Manzanera S, Piers P, Weeber H. Visual effect of the combined correction of spherical and longitudinal chromatic aberrations. *Opt Express*. 2010; 18: 1637–1648. <https://doi.org/10.1364/OE.18.001637> PMID: 20173991
8. Millan S, Vega F. Extended depth of focus intraocular lens: chromatic performance. *Biomed Opt Express*. 2017; 8: 4294–4309. <https://doi.org/10.1364/BOE.8.004294> PMID: 28966865
9. Domínguez-Vicent A, Esteve-Taboada JJ, Del Águila-Carrasco AJ, Ferrer-Blasco T, Montés-Micó R. In vitro optical quality comparison between the Mini WELL Ready progressive multifocal and the TECNIS Symphony. *Graefes Arch Clin Exp Ophthalmol*. 2016; 254: 1387–1397 <https://doi.org/10.1007/s00417-015-3240-7> PMID: 26671689
10. Furlan WD, Andres P, Saavedra G, Pons A, Monsoriu JA, Calatayud A, et al. Inventors Multifocal ophthalmic lens and method for obtaining the same. ES Patent 2011/070559; PCT/ES2014/000094, WO Patent 2012/028755 A1
11. Saavedra G, Furlan WD, Monsoriu JA. Fractal zone plates. *Opt Lett*. 2003; 28: 971–973. PMID: 12836749
12. Monsoriu JA, Furlan WD, Saavedra G, Giménez F. Devil's lenses. *Opt Express*. 2007; 15: 13858–13864. PMID: 19550657
13. Zhang Q, Wang J, Wang M, Bu J, Zhu S, Gao BZ, et al. Depth of focus enhancement of a modified imaging quasi-fractal zone plate. *Opt Laser Technol*. 2012; 44: 2140–2144.
14. Furlan WD, Saavedra G, Monsoriu JA. White-light imaging with fractal zone plates. *Opt Lett*. 2007; 32: 2109–2111. PMID: 17671552
15. Gimenez F, Furlan WD, Calatayud A, Monsoriu JA. Multifractal zone plates. *J Opt Soc Am A*. 2010; 27: 1851–1855.
16. Zhang QQ, Wang JG, Wang MW, Bu J, Zhu SW, Wang R, et al. A modified fractal zone plate with extended depth of focus in spectral domain optical coherence tomography. *J Opt*. 2011; 13: 055301.
17. Furlan WD, Ferrando V, Monsoriu JA, Zagrajek P, Czerwińska E, Szustakowski M. 3D printed diffractive terahertz lenses. *Opt Lett*. 2016; 41: 1748–1751. <https://doi.org/10.1364/OL.41.001748> PMID: 27082335
18. Calatayud A, Monsoriu JA, Mendoza-Yero O, Furlan WD. Polyadic devil's lenses. *J Opt Soc Am A*. 2009; 26: 2532–2537.
19. Monsoriu JA, Saavedra G, Furlan WD. Fractal zone plates with variable lacunarity. *Opt Express*. 2004; 12: 4227–4234. PMID: 19483968
20. Sweeney DW, Sommargren GE. Harmonic diffractive lenses. *Appl. Opt*. 1995; 34: 2469–2475. <https://doi.org/10.1364/AO.34.002469> PMID: 21052382
21. Thibos LN, Hong X, Bradley A, Applegate RE. Metrics of optical quality of the eye. *J. Vis*, 2004; 4, 1–15.
22. Calatayud A, Remón L, Martos J, Furlan WD, Monsoriu JA. Imaging quality of multifocal intraocular lenses: automated assessment setup. *Ophthalmic Physiol Opt*. 2013; 33:420–426. <https://doi.org/10.1111/opo.12063> PMID: 23786382
23. International Organization for Standardization. Ophthalmic implants Intraocular lenses. Optical properties and test methods. (ISO/FDIS 11979–2:2014).
24. Schwiegerling J, Choi J. Application of the polychromatic defocus transfer function to multifocal lenses. *J Refract Surg*. 2008; 24:965–969. PMID: 19044242
25. Remón L, Furlan WD, Monsoriu JA. Multifocal intraocular lenses with fractal geometry. *Opt. Pura Apl*, 2015; 48: 1–8.
26. Nakajima M, Hiraoka T, Yamamoto T, Takagi S, Hirohara Y, Oshika T, et al. Differences of longitudinal chromatic aberration (LCA) between eyes with intraocular lenses different manufactures. *PLoS ONE*. 2016; 11(6):e0156227. <https://doi.org/10.1371/journal.pone.0156227> PMID: 27258141
27. Ravikumar S, Bradley A, Thibos LN. Chromatic aberration on polychromatic image quality with diffractive multifocal intraocular lens. *J Cataract Refract Surg*. 2014; 40: 1192–1204 <https://doi.org/10.1016/j.jcrs.2013.11.035> PMID: 24957438

28. Eppig T, Scholz K, Loffler A, Meßner A, Langenbacher A. Effect of decentration and tilt on the image quality of aspheric intraocular lens designs in a model eye. *J Cataract Refract Surg*. 2009; 35: 1091–1100. <https://doi.org/10.1016/j.jcrs.2009.01.034> PMID: [19465297](https://pubmed.ncbi.nlm.nih.gov/19465297/)
29. Peh S, Fiala W, Malz A, Stork W. In vitro Strehl ratios with spherical, aberration-free, average, and customized spherical aberration-correcting intraocular lenses. *Invest Ophthalmol Vis Sci*. 2009; 50: 1264–1270. <https://doi.org/10.1167/iovs.08-2187> PMID: [18978351](https://pubmed.ncbi.nlm.nih.gov/18978351/)